

Oxide-Free Phosphate Surface Films on Metals Studied by Core and Valence Band X-ray Photoelectron Spectroscopy

John A. Rotole and Peter M. A. Sherwood*

Department of Chemistry, 111 Willard Hall, Kansas State University,
Manhattan, Kansas 66506-3701

Received December 1, 2000. Revised Manuscript Received June 1, 2001

Phosphate films with thicknesses on the order of the original native metal oxide have been formed on oxide-free aluminum and iron surfaces by electrochemical treatment in 5M phosphoric acid. Electrochemistry was performed under inert atmosphere in a previously described anaerobic cell. The metal phosphate films formed under these conditions were studied by core level and valence band X-ray photoelectron spectroscopy (XPS) with the valence band spectra interpreted by spectra generated from band structure calculations. Valence band studies showed that the metal surfaces consisted of a metal phosphate film bonded directly to the metal substrate in the absence of any form of metal oxide. An analysis of the inner valence band region around 25 eV indicates considerable difference between oxidized aluminum and iron compounds and the metal phosphates. The phosphate film initially formed on aluminum is compatible with metaphosphate. This unusual surface is stable in atmosphere and may have significant potential based upon known advantages provided by phosphated surfaces. This study provides a detailed analysis of a recent patent report of oxide free phosphate surface films formed on metal surfaces that are stable under ambient atmosphere.

1. Introduction

The surface of nonnoble metals exist in atmosphere with a native oxide film usually in combination with additional outer surface layers of hydroxide and oxy-hydroxide. If the native oxide is damaged by abrasion or removed in some other fashion the underlying metal will immediately oxidize to reform the oxide. There have been many studies of corrosion films formed on metal surfaces, especially in the case of thick films which can be easily studied by bulk analysis techniques such as X-ray diffraction. In many cases corrosion films are sufficiently thin that ultrahigh vacuum surface analysis probes are needed for their investigation. Some of these studies have examined the role of corrosion inhibitors in surface film modification.^{1–7} A substantial body of literature exists regarding the action of corrosion inhibitors for potential protection of a variety of metal substrates. Corrosion inhibiting treatments lead to a substrate surface that is chemically modified by the inhibitor or the inhibitor can be applied in the form of new or additional protective films placed over the metal oxide. Phosphate containing treatments have a long history of effective action as corrosion inhibitors.

The experiments presented in this study were conducted on two metals, aluminum and iron, with sub-

stantially different reactivities. Aluminum metal, without its protective oxide layer, is highly reactive toward water and oxygen to form a chemically and mechanically stable oxide layer. Thus aluminum metal is generally protected from further atmospheric oxidation by its own native oxide. The high reactivity of aluminum metal imparts a self-healing quality to the protective nature of the oxide. Should the surface film become damaged, the underlying metal will rapidly react to re-form the oxide film. Iron, on the other hand, is much slower to react with water and oxygen to form an oxide layer that is stable chemically but not mechanically. No significant protection from further oxidation is provided by the surface iron oxide which continually flakes away constantly exposing the underlying metal to environmental oxidative agents such as water and oxygen from the atmosphere. This results in the severe material degradation observed for iron.

In planning the appropriate experimental approach for the study of aluminum and iron, it is important to consider the reactive nature of nonnoble metals. To study the interaction of clean, oxide free, metal surfaces with aqueous electrolytes we have designed a special anaerobic cell.⁸ This cell enables a metal to be cleaned free of oxide and contaminants in a ultrahigh-vacuum system, have its surface chemistry monitored, and its surface chemistry altered by aqueous electrolytes with and without the use of electrochemical treatment. It is thus possible to conduct chemistry in an "anaerobic" environment which allows for the possibility of different

(1) Castle, J. E. *Surf. Sci.* **1977**, *68*, 583.

(2) Larson, D. T. *Corros. Sci.* **1979**, *19*, 657.

(3) Joshi, A. *Rev. Coat. Corros.* **1979**, *3*, 51.

(4) Sherwood, P. M. A. *Chem. Soc. Rev.* **1985**, *14*, 1.

(5) Welsh, I. D.; Sherwood, P. M. A. *Chem. Mater.* **1992**, *4*, 133.

(6) Sherwood, P. M. A. *J. Vacuum Sci. Technol. A* **1993**, *11*, 2280.

(7) Liang, Y.; Paul, D.; Sherwood, P. M. A. *Chem. Mater.* **1993**, *5*, 1554.

(8) Liang, Y.; Paul, D.; Xie Y.; Sherwood, P. M. A. *Anal. Chem.* **1993**, *65*, 2276.

reaction outcomes than those possible where the metal surface contains an air-formed oxide film. We have shown in earlier studies⁹ that it is possible to use this approach for the reactive aluminum metal; thus the metal does not form a substantial oxide film during the course of the anaerobic cell operation.

The purpose of this paper is to show that it is possible to change the surface chemistry of both aluminum and iron. We show that it is possible to electrochemically treat aluminum and iron in phosphoric acid to produce a phosphate layer *adjacent* to the metal surface in the *absence of metal oxide*. In this way we form a novel metal surface chemistry which is stable in air. We believe that this new surface preparation may lead to metals with enhanced corrosion resistance. This approach represents a distinct departure from previous spray or dip phosphating treatments in that the original native oxide has been completely removed and replaced by a metal phosphate film that is newly bonded to the metal substrate with a thickness on the same order of magnitude as the original native oxide. The new phosphated surface is free of metal oxide and protects the underlying metal from oxidation in atmosphere. Conclusive evidence regarding the chemical identity of the surface films and the lack of metal oxide is provided by valence band photoemission and supported by core level X-ray photoelectron spectroscopic (XPS) studies. This discovery was recently patented in a U.S. patent (that discussed the iron and aluminum systems in this paper)¹⁰ and reported to occur in copper¹¹ and titanium.¹²

Valence band XPS is very sensitive to the subtle chemical differences commonly found in the multilayer corrosion films of metal surfaces and may be understood by comparing experimental data with spectra predicted by calculation. This approach has been used in our group to understand the complicated nature of many systems including iron,^{5,6,13} aluminum,^{9,14–19} molybdenum,^{20,21} tin,²² and nickel.^{7,8,23} We find in this paper that valence band photoemission is key to proving the presence of phosphate and conclusively distinguishing this from oxide.

2. Experimental Section

2.1. Instrumentation and Anaerobic Cell. XPS measurements were made with a VSW HA150 spectrometer (150

mm hemispherical analyzer), equipped with a 16 plate multichannel detector system, and Al K α X-radiation (240 W) produced from a 32 quartz crystal VSW monochromator providing a line width of better than 0.2 eV. An additional ultrahigh-vacuum chamber designed for solid–liquid interface studies,⁷ which we will refer to as an “anaerobic cell” is separated from the main analysis chamber by a gate valve. The base pressure of the system is better than 10^{–9} Torr. The spectrometer was operated in fixed analyzer transmission (FAT) mode with a pass energy of 44 eV for survey scans and 22 eV for both core level and valence band data. Both the HA150 and the ES200B spectrometer (described below) had their energy scales calibrated using copper²⁴ and spectra were referenced against either the C1s peak of adventitious hydrocarbon at 284.6 eV, or the Fermi edge at 0.0 eV if the presence of a distinct metal edge was observed in the valence band data. Backgrounds were subtracted from some spectra using a previously published method.²⁵

Electrochemical experiments were performed in an anaerobic cell in a specially designed ultrahigh-vacuum chamber, attached to the HA150 XPS instrument, in which electrochemistry and liquid exposure could be performed in the absence of air. The details of this cell have been reported previously.⁷ An important feature of this approach is that it allows the surface of the metal to be cleaned in ultrahigh vacuum, and have its surface chemistry monitored by XPS *before* any electrochemistry or liquid exposure is performed. This feature was essential for the work reported here. In all cases the aluminum or iron sample was cleaned by argon-ion etching, and the XPS spectrum monitored to ensure the absence of any oxide or other contaminant before the electrochemistry was carried out. The experiments used 5 M orthophosphoric acid as the electrolyte. This solution was deoxygenated by saturating the solution with nitrogen gas. Two liquid reservoirs allowed either the phosphoric acid solution or a solution of deoxygenated quadruply distilled water to be added to the anaerobic cell. The water was used for washing the sample after electrochemical experiments, a procedure that was followed in all the experiments reported in this paper.

2.2. Sample Preparation in the Anaerobic Cell. High-purity research metals were used in this study. The 99.9999% aluminum was obtained from Alcan International, and the 99.9975% iron foil was purchased from Alfa Aesar. The samples were degreased with acetone and placed in the anaerobic cell where any native surface oxide was removed by argon ion etching. The Ion Tech B21 saddle field ion etcher employed for this purpose was supplied with 99.99% ultrahigh purity argon from Matheson and was operated at 2 mA and 5 KV with an argon pressure of less than 10^{–3} Torr to yield an etch rate which we estimate to be in the range of 2–5 Å min^{–1}. The aluminum foil was etched for 1.5 h and the iron foil for 4 h until the presence of oxide as monitored in the Al 2p and Fe 2p regions, respectively, and the O 1s region was not detected. While these etching times are long, they ensure that the metal is completely free of oxide and impurities.

2.3. Experimental Procedure Followed in the Anaerobic Cell. Electrochemistry performed in the anaerobic cell was conducted under an inert atmosphere of 99.99% ultrahigh-purity nitrogen from Matheson at positive pressure (>760 Torr) to eliminate contamination from air leaking into the system. The etched aluminum and iron electrodes were polarized for 10 min in 5.0 M phosphoric acid at –0.5 V with respect to a saturated calomel electrode (SCE). After etching, the experiment proceeded as follows: (a) the surface chemistry of the metal surface was monitored by XPS to ensure a clean metal surface; (b) introduction of high-purity nitrogen into the anaerobic cell; (c) placement of the electrochemical cell into the inert atmosphere environment (at a positive pressure); (d) introduction of the 5 M phosphoric acid electrolyte; (e) execution of the 10 min potentiostatic treatment; (f) removal of the

(9) Rotole, J. A.; Sherwood, P. M. A. *Fresenius Z. Anal. Chem.* **2001**, *369*, 342.

(10) Rotole, J. A.; Sherwood, P. M. A. “Metals Having Phosphate Protective Films. U.S. Patent No. 6, 066, 403, May 23, 2000.

(11) Rotole, J. A.; Sherwood, P. M. A. *J. Vacuum Sci. Technol. A* **2000**, *18*, 1066.

(12) Rotole, J. A.; Gaskell, K.; Comte, A.; Sherwood, P. M. A. *J. Vacuum Sci. Technol. A* **2001**, *19*, 1176.

(13) Welsh, I. D.; Sherwood, P. M. A. *Phys. Rev. B* **1989**, *40*, 6386.

(14) Thomas, S.; Sherwood, P. M. A. *Anal. Chem.* **1992**, *64*, 2488.

(15) Thomas, S.; Sherwood, P. M. A. *J. Chem. Soc., Faraday Trans.* **1993**, *89*, 263.

(16) Rooke, M. A.; Rotole, J. A.; Sherwood, P. M. A. *J. Vacuum Sci. Technol. A* **1995**, *13*, 1299.

(17) Havercroft, N.; Sherwood, P. M. A. *J. Vacuum Sci. Technol. A* **1998**, *16*, 1112.

(18) Sherwood, P. M. A. *Surf. Sci. Spectra* **1998**, *5*, 1.

(19) Rotole, J. A.; Sherwood, P. M. A. *J. Vac. Sci. Technol. A* **1999**, *17*, 1122.

(20) Hixson, H.; Sherwood, P. M. A. *J. Chem. Soc., Faraday Trans.* **1995**, *91*, 3593.

(21) Hixson, H.; Sherwood, P. M. A. *Chem. Mater.* **1996**, *8*, 2643.

(22) Sherwood, P. M. A. *Phys. Rev. B* **1990**, *41*, 10151.

(23) Liang, Y.; Paul D.; Sherwood, P. M. A. *J. Chem. Soc., Faraday Trans.* **1994**, *90*, 1271.

(24) Seah, M. P.; Gilmore, I. S.; Beamson, G. *Surf. Interface Anal.* **1998**, *26*, 642.

(25) Proctor, A.; Sherwood, P. M. A. *Anal. Chem.* **1982**, *54*, 13.

electrolyte and electrochemical cell from the anaerobic cell with the potentiostat switched on; (g) washing of the sample with quadruply distilled water by filling the cell with water, and then immediately draining the cell (which takes about 1 min); and (h) reestablishment of the original ultrahigh-vacuum environment. This process took roughly 30 min.

2.4. Conventional Electrochemical Experiments and Surface Analysis. XPS studies of samples from experiments involving electrochemistry carried out in a conventional electrochemical cell, with the sample transferred in air to the spectrometer were performed on an AEI Kratos ES200B X-ray photoelectron spectrometer. The spectrometer is equipped with a 127 mm radius hemispherical analyzer, a Mg K α (240 W) radiation source, a single-channel electron multiplier, and had a base pressure of 10^{-9} Torr. The spectrometer was operated in fixed retardation ratio (FRR) mode (1:23) with a resolution on the same order as the X-ray line width (0.8 eV).

Conventional electrochemical treatments were performed in a standard glass electrochemical cell which has been described previously²⁶ operated on the laboratory bench. All the solutions used deoxygenated quadruply distilled water. All electrochemical treatments were conducted with a Thompson Electrochem Ltd. Ministat Research Potentiostat Model No.402R made in Newcastle upon Tyne (U.K). In all electrochemical experiments the electrodes were removed from the electrolyte with the potentiostat switched on. All electrolytes were deoxygenated by bubbling with nitrogen gas.

2.5. XPS Measurements of Standard Compounds. The XPS spectra of the pure oxide and phosphate substances were obtained from research grade powder samples recorded on the VSW HA150 instrument with monochromatic X-radiation using the spectrometer conditions described above. The corundum (α -Al₂O₃), iron oxide and oxyhydroxide powders from Alfa, the aluminum metaphosphate and the aluminum phosphate powders from Aldrich, and the iron phosphate samples from Pfalz and Bauer were spread on double sided tape and mounted on a copper sample carrier. Surface charging was negated with a low-energy electron flood gun operated at 2.20 A and 275 V (the manufacturer's recommended settings) during spectral collection. No signal from the copper sample carrier was detected during XPS analysis.

2.6. Calculations. The valence band spectrum of the phosphate and metaphosphate ions was interpreted using data obtained from band structure calculations and from cluster calculations using the traditional Hartree–Fock approach. The band structure calculations were carried out using an extended version of the program CRYSTAL.^{27,28} Calculations were performed for the *R3c* structure of α -Fe₂O₃,²⁹ the *Pbnm* structure of α -FeOOH,^{30,31} the rhombohedral structure of α -Al₂O₃,³² the *C222₁* structure and the *P3₂2* structure (berlinite) of AlPO₄,³³ the *T_h^h* structure of Al₄(P₄O₁₂)₃ (aluminum metaphosphate (Al(PO₄)₃)),³² the *P2₁/n* structure of gibbsite (Al(OH)₃),³⁴ and the *P3₂2* structure of FePO₄·2H₂O (strengite).³³ The basis set of Wachters³⁵ was used for iron and the STO-3G basis set used for aluminum and oxygen. All the calcula-

tions were restricted Hartree–Fock (RHF) calculations. Calculated spectra were generated from the band structure by adjusting the density of states in the valence band for each orbital symmetry type (O 2s and O 2p, P 3s and P 3p, Al 3s, Fe 4s, Fe 3d) by the appropriate Scofield atomic photoelectron cross-section.³⁵ In the case of the calculations for the iron compounds the O 2s cross-section was reduced to 50% of the Scofield value; using this value gives better agreement with the experimental area ratio in the O 2s and O 2p regions, though the spectral appearance is not markedly changed by doing this.³⁷ The density of states was then convoluted with a 50% mixed Gaussian–Lorentzian product function with a full width at half-maximum (fwhm) of 1 eV for the iron compounds and 1.5 eV for the aluminum compounds.^{38–40} The aluminum calculations in Figure 2 use a fwhm of 3.0 eV with the energy scale contracted by 1.3.

3. Results and Discussion

3.1. Types of Experiments Performed. Four types of experiments were conducted on iron and aluminum foils and are shown in the following figures indicated (E1–E4) in the order listed here. Experiment 1 (E1) involved the 10 min polarization in the phosphoric acid electrolyte conducted under inert atmosphere in the anaerobic cell described below. To test the stability of the resulting surface film against atmospheric oxidation, the sample of experiment 1 was exposed to atmosphere followed by a second XPS analysis in experiment 2 (E2). In experiment 3 (E3) the sample was subjected to electrochemistry carried out in a conventional electrochemical cell, with the sample transferred in air to the spectrometer. The metal samples used were the “as received” metal foils with their air formed oxide films, and these samples were subjected to an electrochemical treatment identical to that of experiment 1. Experiment 4 (E4) was performed in the anaerobic cell, using the same procedure as experiment 1, except that quadruply distilled water was used instead of 5 M orthophosphoric acid and no electrochemical treatment was conducted.

3.2. Electrochemical Treatment of Aluminum in Phosphoric Acid. In this section the results of core level spectra will be discussed first, which gives an initial view of the changes occurring, but it will be seen that the valence band spectra yield the most important information about the chemical changes caused by the sequence of experiments discussed above.

3.2.1. Core Level Spectra. The Al 2p, P 2p, and O 1s spectra for the set of experiments conducted on aluminum are shown in Figure 1.

The Al 2p region shows two principal features, a metal peak around 72 eV and a wider peak around 75 eV. As pointed out in our previous work,^{14,18} there are only small differences between the metal binding energy on one hand and aluminum compounds on the other hand. In particular the Al 2p binding energies of the oxides are very similar to those of the phosphates (AlPO₄ and Al(PO₃)₃) lying in a binding energy range of only around

(26) Dickinson, T.; Povey, A. F.; Sherwood, P. M. A. *J. Chem. Soc., Faraday Trans. 1* **1975**, *71*, 298.

(27) Pisani, C.; Dovesi, R.; Roetti, C. *Hartree–Fock ab Initio Treatment of Crystalline Systems*; Lecture Notes in Chemistry, 48; Springer: Berlin, 1988; and QCPE 577.

(28) Saunders, V. R.; Dovesi, R.; Roetti, C.; Causà, M.; Harrison, N. M.; Orlando, R.; Zicovich-Wilson, C. M. *Crystal 98 User's Manual*; University of Torino: Turin, Italy, 1998.

(29) Blake, R. L.; Zoltai, T.; Hessevick, R. E.; Finger, U. W. *U. S., Bur. Mines Rep. Invest.* **1970**, No. 7384.

(30) Szytula, A.; Burewicz, A.; Dimitrijević, Z.; Krasnicki, S.; Rany, H.; Todorović, Wanic, A.; Wolski, W. *Phys. Stat. Sol.* **1968**, *26*, 429.

(31) Sampson, C. F. *Acta Crystallogr.* **1969**, *B25*, 1683.

(32) Wyckoff, R. W. G. *Crystal Structures*, 2nd. ed.; Wiley: New York, 1964; Vol. 2.

(33) Wyckoff, R. W. G. *Crystal Structures*, 2nd. ed.; Wiley: New York, 1965; Vol. 3.

(34) Saalfeld, H.; Wedde, M. Z. *Kristallogr.* **1974**, *139*, 129.

(35) Wachters, A. J. H. *J. Chem. Phys.* **1970**, *52*, 1033.

(36) Scofield, J. H. *J. Electron Spectrosc. Relat. Phenom.* **1976**, *8*, 129.

(37) Hixon, H. H.; Sherwood, P. M. A. *J. Phys. Chem. B* **2001**, *105*, 3957.

(38) Ansell, R. O.; Dickinson, T.; Povey, A. F.; Sherwood, P. M. A. *J. Electroanal. Chem. Interfacial Electrochem.* **1979**, *98*, 79.

(39) Sherwood, P. M. A. In *Practical Surface Analysis by Auger and Photoelectron Spectroscopy*; Briggs, D., Seah, M. P., Eds.; Wiley: London, 1983; p 445.

(40) Sherwood, P. M. A. In *Practical Surface Analysis by Auger and Photoelectron Spectroscopy*, 2nd. ed.; Briggs, D., Seah, M. P., Eds.; Wiley: London, 1990; Vol. 1, p 555.

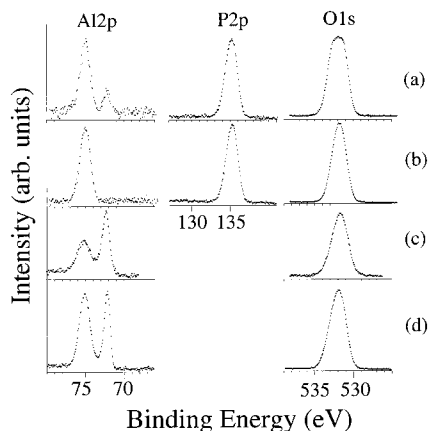


Figure 1. Core X-ray photoelectron spectra of the Al 2p, P 2p, and O 1s spectra of (a) the film formed on aluminum metal after treatment in 5 M orthophosphoric acid in the anaerobic cell for 10 min (E1), (b) the film in a after exposure to the atmosphere for 2 weeks (E2), (c) the film formed on as received aluminum metal in 5 M orthophosphoric acid on the bench (E3), and (d) the film formed on aluminum metal after exposure to deoxygenated water in the anaerobic cell for 10 min (E4).

0.8 eV, with a difference of less than 0.5 eV between the orthophosphate (AlPO_4) and the metaphosphate ($\text{Al}_4(\text{P}_4\text{O}_{12})_3$).^{18,41,42} The P 2p region in experiments 1 and 2 show a P 2p peak around 135 eV, as expected for these phosphate compounds. The fwhm of the P 2p peak and in particular the O 1s peak was less in experiment 2 than in experiment 1. This is compatible with the differences seen for orthophosphate and metaphosphate.^{41,42} In the case of metaphosphate a broad O 1s region is expected because of the two different types of oxygen in the cyclic metaphosphate ion. When one considers the possibility of differential sample charging which can arise when one has a thin layer of insulating aluminum compound on top of a conducting metal oxide, any small errors that could arise from this source makes the use of core Al 2p binding energies of little value in determining the changes that have occurred. It is important to note that differential charging will not seriously impact our valence band region analysis because in this analysis (discussed below) the changes in the relative peak positions and peak appearance are normally the most significant diagnostic feature. In particular what we can say with certainty is that experiment 1 leads to the formation of a film of an aluminum compound on the surface and that this compound thickens after air exposure in experiment 2 to give a layer that is sufficiently thick that the underlying metal cannot be seen.

It is clear that the experiment on the bench (experiment 3) leads to a thinning of the normal air formed oxide film¹⁸ (the as received film gives an Al 2p region similar to Figure 1a). We believe that nearly all the Al 2p intensity around 75 eV is due to oxide and not phosphate based upon the low P 2p intensity. Some P 2p intensity was noted, but is not shown in Figure 1c because of its low intensity and resulting poor statistics. The phosphorus to aluminum (based upon P 2p/Al 2p)

atomic ratios can be obtained on the basis of the gross approximation that the surface region probed is uniform. The ratios are based upon the area of the Al 2p aluminum compound peak around 75 eV and the P 2p peak. These ratios were adjusted by the photoelectron cross-sections due to Scofield³⁶ and adjusted for the spectrometer transmission function. The area ratio for experiment 1 is 2.17 and shows a ratio that is consistent with a film composition of aluminum metaphosphate ($\text{Al}_4(\text{P}_4\text{O}_{12})_3$) (which would have a ratio of 3). The area ratio for experiment 2 shows a decrease in the P/Al ratio to 1.80 consistent with a film composition of aluminum phosphate film (AlPO_4) (which would have a ratio of 1). The area ratio for experiment 3 showed a small amount of phosphorus corresponding to a P/Al ratio of about 0.2 consistent with a small amount of phosphate ion adsorbed on an oxide film. Bearing in mind the errors involved in the area ratio approach, what one can see is a fall in the amount of phosphorus to aluminum consistent with the conversion of metaphosphate to phosphate. Uncertainties associated with the area ratio approach, especially if the phosphorus is nonuniformly located in the surface, means that we cannot place too much reliance on these ratios for the identification of metaphosphate. We believe that the principal evidence for the presence of metaphosphate is provided by the valence band XPS data. Atomic ratios using the O 1s region are of little value because there are additional sources of oxygen such as chemisorbed oxygen and chemisorbed water.

In Figure 1d the spectra from experiment 4 shows the formation of a thin oxide film with Al 2p features of equal intensity. This indicates that the reaction in experiment 1 is much more rapid than in experiment 4 because both experiment 1 and experiment 4 were conducted for identical liquid exposure times, so the formation of the metaphosphate film under the imposed electrochemical conditions is more rapid than the formation of oxide under open circuit potential.

An estimate of the film thicknesses may be made on the basis of the area ratio of the Al 2p core level features for the metal and metal compounds if one makes the crude assumption that the sample is composed of a uniform homogeneous film on top of the metal.^{9,43–46} Using this assumption and assuming an “average” oxidized aluminum species in experiments 3 and 4, the thickness of the layer can be taken to be about 15 Å in experiment 3 and about 25 Å in experiment 4. In the case of the initially formed metaphosphate layer the thickness is probably in the range of 80–100 Å (based on the low atomic density of aluminum in the metaphosphate (which is about 10% aluminum by weight)).

3.2.2. Valence Band Spectra. Conclusive evidence for the chemical identity of the surface films formed in these experiments is provided by valence band photoemission. Valence band XPS may distinguish between compounds which are chemically very similar. Such compound specificity is often not available in the core level but arises in the valence band as a result of bonding interactions of the valence electrons. Analysis of this region provides bonding information about the specific solid and thus the spectral shape is often unique to the compound concerned. Since one can never be certain if the surface composition of a material varies

(41) Rotole, J. A.; Sherwood, P. M. A. *Surf. Sci. Spectra* **1998**, *5*, 67.

(42) Rotole, J. A.; Sherwood, P. M. A. *Surf. Sci. Spectra* **1998**, *5*, 60.

from its bulk composition, the approach taken is to compare experimental XPS spectra to spectra predicted by appropriate calculation methods.

Before discussing the results of our four experimental approaches, it is useful to discuss the spectral features found for phosphate compounds because the analysis of the core region suggests that such compounds can be formed in our experimental sequence, and it is important to demonstrate that these phosphate compounds can be distinguished from one another and from oxidized aluminum compounds.

3.2.2.1. Inner Valence Band Region. A key consideration in the analysis of the experiments reported in this paper is to identify whether the films formed contain oxide, especially on exposure of the films formed on the metal after exposure to the air. The core region is not conclusive in making this determination because both oxide and phosphate give peaks in the Al 2p region in the vicinity of 75 eV as discussed above. In particular it is important to determine whether exposure of the film formed in the anaerobic cell to the atmosphere leads to formation of oxide, or as we will indicate below, the formation of orthophosphate. The Al 2p region shows a change (Figure 1a compared with Figure 1b), which would be compatible with either interpretation. We have reported the overall valence band region in our patent documents.¹⁰ Superficial examination of the inner valence band region around 25 eV, the region where principally O 2s features are seen in oxides and phosphates, and P 3s features in phosphates appear similar with a single peak with variations in peak width and peak symmetry. Closer examination of this region shows significant differences, both between different oxidized species and between oxidized species and phosphates. Figure 2 shows the inner valence band region for the film formed in the anaerobic cell (a-1), the difference between this film and aluminum metaphosphate ((Al₄(P₄O₁₂)₃) (a-2), which indicates that these spectra are nearly identical (the areas of the two spectra are within 0.2% of each other). The very similar spectrum for the film formed after exposure of the film formed in the anaerobic cell to the atmosphere for 2 weeks is shown in b and the same region in different oxidized aluminum species in the rest of the figure. The spectra of the oxidized aluminum species and aluminum orthophosphate are taken from our previously reported valence band spectra obtained with monochromatic X-radiation.^{18,19,42,47-53} One notes that the oxidized aluminum species in c, d, g, and h show a single peak consistent

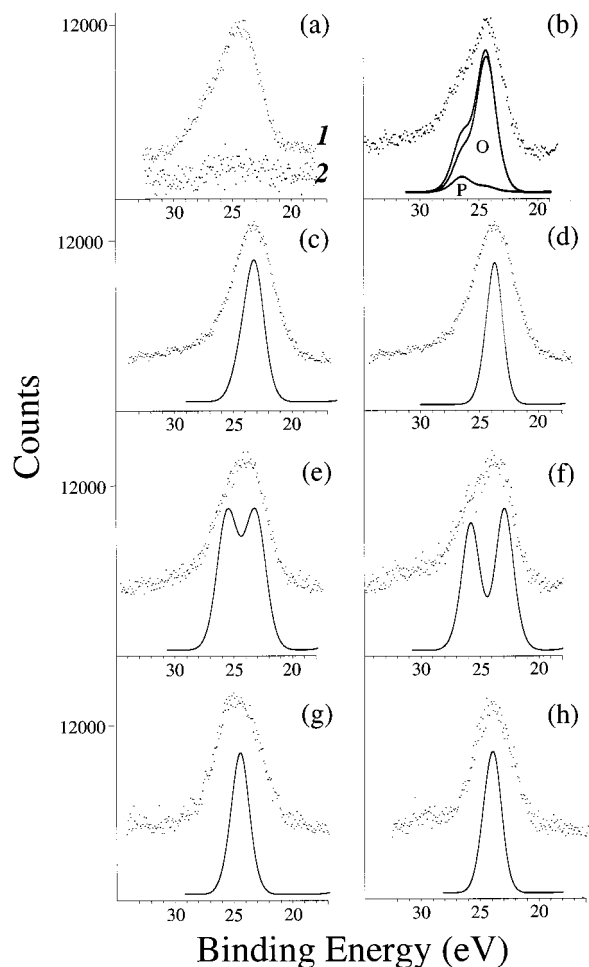


Figure 2. Background subtracted outer valence band region of (a) the film formed after treatment in the anaerobic cell (in 1) and the difference between this spectrum and the spectrum of aluminum metaphosphate ((Al₄(P₄O₁₂)₃) (in 2), (b) the film formed after treatment in the anaerobic cell and exposure to the atmosphere for 2 weeks, (c) α -Al₂O₃, (d) γ -Al₂O₃, (e) AlOOH (boehmite), (f) AlOOH (diaspore), (g) Al(OH)₃ (bayerite), and (h) Al(OH)₃ (gibbsite). Calculated spectra from band structure calculations are shown inserted into the figure. In the case of a and b the calculated valence band spectra for AlPO₄ are shown with the intensity due to oxygen (O) and phosphorus (P) identified.

with the oxide oxygens in c and d and the hydroxide oxygens in g and h. The spectra generated from band structure calculations predict this observation. The spectrum of aluminum orthophosphate and the spectrum of the surface formed after exposure of the film formed in the anaerobic cell to the atmosphere appear identical (as indicated by the difference spectrum in Figure 3), and show two features, with a clear high binding energy shoulder. The spectrum predicted from band structure calculations shows that this shoulder arises from P–O orbitals of the phosphate ion. The spectra of the oxyhydroxides of aluminum e and f show the broadest spectrum consistent with two features predicted (but not resolved in the experimental data) from the band structure calculations. The ability of this region to distinguish between oxidized aluminum species and aluminum orthophosphate is indicated by the difference spectra shown in Figure 3. Thus while the difference spectrum between the surface formed after exposure of the film formed in the anaerobic cell to the

(43) Strohmeier, B. R. *Surf. Interface Anal.* **1990**, *15*, 51.

(44) Gunter, P. L. J.; de Jong, A. M.; Niemantsverdriet, J. W.; Rheiter, H. J. H. *Surf. Interface Anal.* **1992**, *19*, 161.

(45) Carlson, T. A. *Surf. Interface Anal.* **1982**, *4*, 125.

(46) Strohmeier, B. R. *J. Vacuum Sci. Technol. A* **1989**, *7*, 3238.

(47) Rotole, J. A.; Sherwood, P. M. A. *Surf. Sci. Spectra* **1998**, *5*, 11.

(48) Rotole, J. A.; Sherwood, P. M. A. *Surf. Sci. Spectra* **1998**, *5*, 18.

(49) Rotole, J. A.; Sherwood, P. M. A. *Surf. Sci. Spectra* **1998**, *5*, 25.

(50) Rotole, J. A.; Sherwood, P. M. A. *Surf. Sci. Spectra* **1998**, *5*, 32.

(51) Rotole, J. A.; Sherwood, P. M. A. *Surf. Sci. Spectra* **1998**, *5*, 39.

(52) Rotole, J. A.; Sherwood, P. M. A. *Surf. Sci. Spectra* **1998**, *5*, 46.

(53) Rotole, J. A.; Sherwood, P. M. A. *Surf. Sci. Spectra* **1998**, *5*, 53.

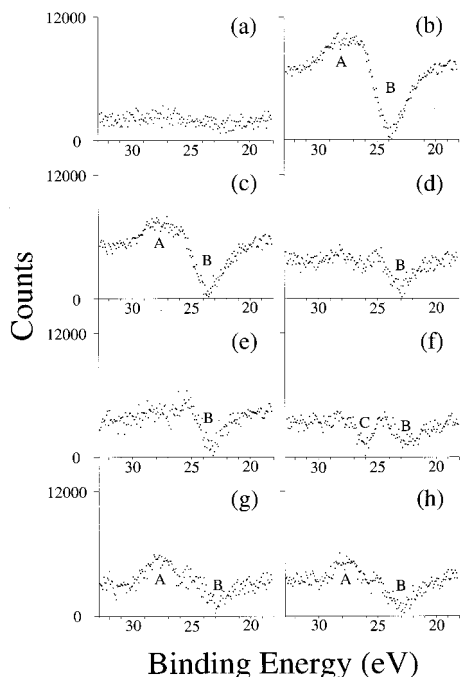


Figure 3. Difference spectra between the spectrum of the film formed after treatment in the anaerobic cell and exposure to the atmosphere for 2 weeks and other spectra and the spectrum of the species identified in a–h below. Each background subtracted spectrum was adjusted so that the most intense point in the spectrum was set to 10 000 counts. The spectrum subtracted is (a) AlPO_4 , (b) $\alpha\text{-Al}_2\text{O}_3$, (c) $\gamma\text{-Al}_2\text{O}_3$, (d) AlOOH (boehmite), (e) AlOOH (diaspore), (f) $\text{Al}(\text{OH})_3$ (bayerite), (g) $\text{Al}(\text{OH})_3$ (gibbsite), and (h) $\text{Al}(\text{OH})_3$ (nordstrandite). Regions A–C are identified in the text.

atmosphere and aluminum orthophosphate indicates that these spectra are the same, there are considerable differences between this spectrum and the oxidized aluminum species. One notes three features in the difference spectra, identified as A–C. Feature A arises from the P–O shoulder at around 28 eV in the orthophosphate spectra, which is absent from the spectra of the oxides. Feature B arises from the difference in the binding energy and width of the principally O 2s region in the oxides and those of the phosphate (the difference in binding energy being greatest for $\alpha\text{-Al}_2\text{O}_3$ (about 1.2 eV) and least for gibbsite (about 0.2 eV)¹⁸). Feature C arises from differences in width of the region for the wider bayerite spectrum (Figures 2g and 3f). Feature A is not observed for the difference spectra (Figure 3d,e) of the wide oxyhydroxide spectra (Figure 2e,f) which show intensity in the same region as the P–O region of the orthophosphate.

3.2.2.2. Phosphate Valence Band Spectra. The spectra of phosphate compounds have been extensively investigated theoretically and experimentally (see ref 5 and references cited therein and refs 40 and 41). Figure 4 presents experimental and calculated spectra of a typical aluminum oxide ($\alpha\text{-Al}_2\text{O}_3$) and two forms of aluminum orthophosphate (AlPO_4) and aluminum metaphosphate ($\text{Al}_4(\text{P}_4\text{O}_{12})_3$). The “berlinite” form of aluminum orthophosphate spectrum will be discussed in section 3.2.2.3. Three peak positions are identified in Figure 4c. Peak 1, at 16 eV is the highest binding energy peak of the metaphosphate ion. Peak 2, at 14 eV, is the highest binding energy peak of the orthophosphate ion, and peak 3, at 11 eV, is the second highest binding

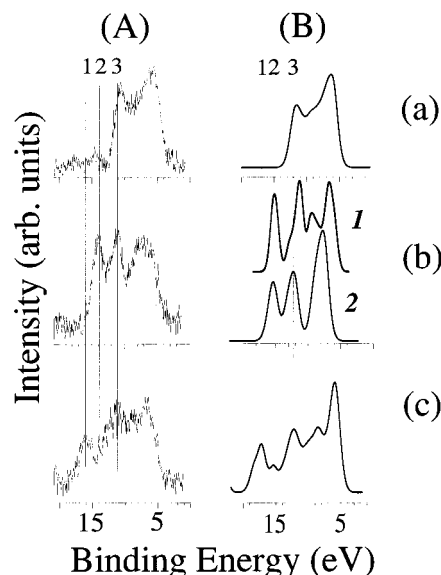


Figure 4. (A) Experimental valence band X-ray photoelectron spectra and (B) spectra calculated from band structure calculations of (a) $\alpha\text{-Al}_2\text{O}_3$, (b) aluminum orthophosphate (AlPO_4), where **1** corresponds to the form known as berlinite and **2** corresponds to the form with the gallium phosphate structure, and (c) aluminum metaphosphate ($\text{Al}_4(\text{P}_4\text{O}_{12})_3$). The experimental spectra were background subtracted.

energy peak in both the metaphosphate ion and the orthophosphate ion. The spectrum of $\alpha\text{-Al}_2\text{O}_3$ is an example of an aluminum oxide valence band spectrum. The aluminum oxides, hydroxides, and oxyhydroxides show significant differences in the valence band region,^{14,19} but the range of energies in the valence band region for these other compounds is typified by $\alpha\text{-Al}_2\text{O}_3$. It is important to note that peaks 1 and 2 (Figure 4) lie at a binding energy *higher* than any of the aluminum oxides, hydroxides, or oxyhydroxides. It is thus possible to unambiguously distinguish between the presence of phosphate and metaphosphate on one hand and oxidized aluminum compounds on the other hand. In the symmetrical orthophosphate ion there are two narrow and distinct and approximately equal intensity phosphate peaks at 11 and 14 eV. In the lower symmetry metaphosphate ion there are two broader, and more widely separated, features at 11 and 16 eV, with the lower binding energy peak being more intense. Both phosphate and metaphosphate have a low binding energy peak near 7 eV.

It is important to establish whether the differences seen between orthophosphate and metaphosphate are reasonable, bearing in mind that any standard compound may contain a surface which is different from the bulk or may have been altered by examination at ultrahigh vacuum and or by X-ray exposure. We have thus calculated the valence band spectra for the phosphate and metaphosphate compounds, and $\alpha\text{-Al}_2\text{O}_3$. The calculated spectra were contracted by a factor of 1.3—a common practice for calculations using the simple STO-3G basis set. Despite this simple basis set, the aluminum metaphosphate calculation was a substantial one involving 104 atoms in the unit cell and 287 valence orbitals. It is clear that the calculations, all of which use the same basis set, predict the same ordering of the peaks 1, 2, and 3 shown experimentally.

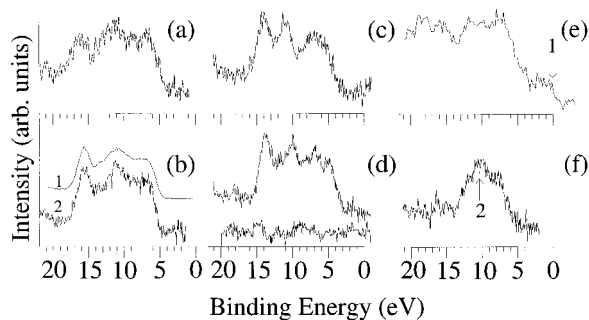
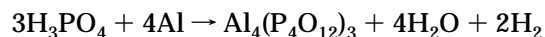


Figure 5. Valence band X-ray Photoelectron Spectra of (a) aluminum metaphosphate ($\text{Al}_4(\text{P}_4\text{O}_{12})_3$), (b) the film formed on argon ion etched aluminum metal after treatment in 5 M orthophosphoric acid in the anaerobic cell (E1) (1 is the spectrum for the film formed at the rest potential, and 2 is the spectrum for the film formed at -0.5V), (c) the outer valence band region of AlPO_4 , (d) the film in a after exposure to the atmosphere for 2 weeks (E2) with the difference spectrum between this spectrum and that of c shown below the spectrum, (e) the film formed on as received aluminum metal in 5 M orthophosphoric acid on the bench (E3), and (f) the film formed on argon-ion etched aluminum metal after exposure to deoxygenated water in the anaerobic cell for 10 min (E4). In e the arrow 1 points to the aluminum metal edge. In f the arrow 2 points to the $\text{Ar}3p$ feature from the underlying metal.

The energy bands (binding energy plotted against wave vector \mathbf{k}) for the outer valence energy levels for selected directions in the first Brillouin zone for aluminum metaphosphate ($\text{Al}_4\text{P}_4\text{O}_{12}_3$), aluminum orthophosphate (AlPO_4), and iron(III) phosphate ($\text{FePO}_4 \cdot 2\text{H}_2\text{O}$) are all quite flat, indicating that the spectrum associated with the phosphate ion (PO_4^{3-}) and the metaphosphate ion ($\text{P}_4\text{O}_{12}^{4-}$) are likely to be similar in compounds with different cations. Comparison of the two orthophosphates of aluminum and iron shows some greater dispersion in the case of the aluminum compound but very similar energy ranges. Indeed the appearance of the phosphate ion spectrum in the two phosphates appears similar with the distinctive features around 14 and 11 eV. The calculated spectra presented in this paper for the two orthophosphates is similar to the calculated spectra for the orthophosphate ion from multiple scattered wave X α calculations reported earlier.⁵

3.2.2.3. Valence Band Spectra Seen in the Sequence of Four Experiments. The valence band spectrum of the film formed in the anaerobic cell using experimental approach 1 is presented in Figure 5b-2. This spectrum shows close agreement with the spectrum obtained for an aluminum metaphosphate powder sample spectrum in Figure 5a, clearly showing that the film formed in the anaerobic cell is consistent with aluminum metaphosphate. Furthermore, when Figure 5b-2 is compared with the valence band spectrum of a typical oxide (Figure 5a), there is no support for the presence of oxide in the valence band spectrum (for the reasons discussed above in the discussion of Figure 5), indicating that the metaphosphate film is in the unusual state of *being bonded directly to the aluminum surface*. This process may involve the formation of the metaphosphate ion in a process such as



leading to the formation of aluminum metaphosphate ($\text{Al}_4(\text{P}_4\text{O}_{12})_3$) bonded directly onto the metal surface. We believe that it is important to perform this process at a relatively negative potential to prevent the formation of oxide on the surface. In fact in the case of aluminum we find that the rest potential for the as received metal is in the same range as the conditions used electrochemically (we measured the rest potential as being -0.62V). We repeated the experiment in the anaerobic cell at the rest potential rather than under -0.5V polarization and find an identical valence band spectrum (Figure 5b-1).

Of course there are a large number of condensed phosphates, and we have chosen the metaphosphate spectrum for comparison with our initially formed films because of the considerable similarities in the spectra, but we cannot rule out the possibility that the phosphate film formed corresponds to another condensed phosphate.

A similar comparison is made of the valence band data for the aluminum phosphate sample in Figure 5c to that of the film formed in the anaerobic cell after two weeks in laboratory atmosphere (experiment 2) shown in Figure 5d. The spectrum is clearly different from the expected spectrum for aluminum metaphosphate, while comparing well to the spectrum of aluminum phosphate. Figure 5d also shows the difference spectrum between Figure 5c,d, showing no significant difference when the spectral statistics are considered. It is interesting to note that the area of the whole valence band region (inner and outer) for aluminum orthophosphate and the film formed after treatment in the anaerobic cell and exposure to the atmosphere for 2 weeks is almost identical with a difference of less than 1%. Despite the close similarities of the two spectra, it is interesting to consider small differences. One notes that Figure 5d shows a valley at 6 eV which suggests that there is a feature present at 5 eV, indeed that Figure 5d is really a four peak structure. Consistent with this approach is the smaller valley between the peak around 11 eV and the lower binding energy feature. One also notes a slightly larger separation between the peaks around 11 eV and 14 eV in Figure 5d compared with Figure 5c, with the former showing peaks at 14 and 11 eV and the latter showing peaks at 14 and 10.2 eV. To investigate this matter further, we calculated the predicted valence band spectrum of another crystalline form of aluminum orthophosphate known as berlinite. The calculated spectrum (Figure 4b-1) does show four features, an increased separation between features 2 and 3, and a smaller valley between the second and third peaks. While we cannot determine with certainty what the actual surface crystallography might be for such thin films, it can be seen that it is quite reasonable for the differences between Figure 5c,d to be explained by different crystal forms of aluminum orthophosphate. This explanation is consistent with the nearly identical areas for the two spectra, because the composition would be unchanged when the crystal form was changed. It is not possible to explain the result by the presence of oxide because of the changes in the relative areas that would result and the changes that would necessarily result in the inner valence band region and which are not observed in this region (*vide supra*). There is thus

no evidence for the presence of oxide in the spectrum; thus this *air stable* phosphate film is also bonded, attached to the metal without any intervening oxide. The aluminum metaphosphate film has clearly been converted to aluminum phosphate by the conditions of experiment 2. It is possible to explain this conversion by the process indicated below, where the metaphosphate ion is converted to the orthophosphate ion:

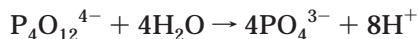


Figure 5e presents the valence band data for the sample subjected to electrochemistry carried out in a conventional electrochemical cell, with the sample transferred in air to the spectrometer (experiment 3), and the 10 min deoxygenated water dip of etched aluminum in the anaerobic cell (experiment 4) is given in Figure 4f. Clearly the films formed in these situations are oxide in nature rather than phosphate. The standard two peak structure below 15 eV characteristic of oxidized aluminum is clearly present in both spectra, and no distinctive phosphate features are present. Figure 4e shows some C 2s intensity at a binding energy greater than 15 eV, plus some underlying metal indicated by the metal edge identified as 1.

Experiment 4 shows a valence band spectrum characteristic of oxidized aluminum plus some argon 3p intensity identified by the feature identified as 2. The argon 3p feature arises as a result of the argon implanted into the metal during the initial oxide removal via argon ion etching. The argon 3s/3p features could be removed via spectral subtraction to identify the oxide film.⁹ In experiment 3 one notes that the oxide film is *thinned* in contrast to experiment 1 where no oxide film is seen but a metaphosphate film is formed directly on the metal with no included oxide.

3.3. Electrochemical Treatment of Iron In Phosphoric Acid. The set of experiments a–d were conducted with iron foil samples. As with the aluminum, the valence band spectra of iron yield the most important information regarding the surface chemistry of this system.

3.3.1. Core Level Spectra. The Fe 2p, P 2p, and O 1s spectra for the set of experiments conducted on aluminum are shown in Figure 6.

The Fe 2p region shows two principal features in the Fe 2p_{1/2} and the Fe 2p_{3/2} region, a metal peak around 706.8 eV and a wider peak around 711 eV in the Fe 2p_{3/2}. The binding energies for the common oxides of iron are 710.1 eV for Fe₃O₄, 710.7 eV for α-Fe₂O₃, and 711.4 eV for FeOOH.¹³ The binding energy for FePO₄·2H₂O is 711.4 eV, which takes a value of around 711 eV in Fe₃(PO₄)₂·8H₂O.⁵ In the case of iron, as in aluminum, it is thus not possible to distinguish between oxidized iron and iron phosphate on the basis of Fe 2p binding energy. The O 1s region shows an oxide peak around 529.5 eV, a hydroxide peak around 531.5 eV, and some adsorbed water around 533.5 eV. The phosphate features occur around 531.5 eV.

In experiment 1 a substantial amount of phosphate is predicted on the basis of the valence band studies discussed below, showing a peak at about 711 eV in addition to the metal peak around 707 eV. In experiment 2, air exposure clearly leads to a thickening of this film with a substantial reduction in the metal peak

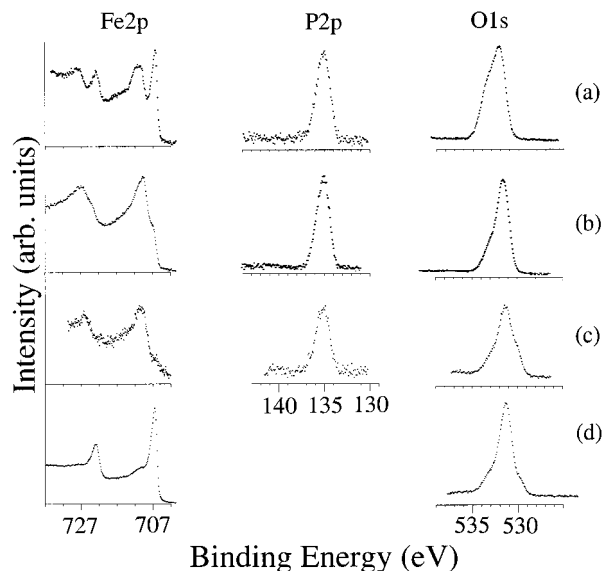


Figure 6. Core X-ray photoelectron spectra of the Fe 2p, P 2p, and O 1s spectra of (a) the film formed on argon ion etched iron metal after treatment in 5 M orthophosphoric acid in the anaerobic cell (E1), (b) the film in air after exposure to the atmosphere for 3 months (E2), (c) the film formed on as received iron metal in 5 M orthophosphoric acid on the bench (E3), and (d) the film formed on argon-ion etched iron metal after exposure to deoxygenated water in the anaerobic cell for 10 min (E4).

intensity. No discoloration of the sample was observed. The bench experiment 3 shows very little metal. We believe that nearly all the Fe 2p intensity around 711 eV is due to oxide and not phosphate based upon the low P 2p intensity.

In Figure 6d the spectra from experiment 4 shows the formation of a very thin oxide film with the Fe 2p region dominated by the metal. The smaller amount of oxide formed compared with the aluminum case is consistent with the much lower reactivity of iron compared with aluminum. As in the aluminum case this indicates that the reaction in experiment 1 is much more rapid than in experiment 4 (even more so than in the aluminum case), so the formation of the phosphate film under the imposed electrochemical conditions is more rapid than the formation of oxide under open circuit potential.

The P 2p region in experiments 1–3 show a P 2p peak around 135 eV, as expected for phosphate. The fwhm of the P 2p peak and the O 1s peak was comparable in experiments 1 and 2. The P 2p peak intensity was of much lower intensity in the case of experiment 3 as found for the aluminum case.

The phosphorus to iron (based upon P 2p/Fe 2p) atomic ratios can be obtained based upon the gross approximation that the surface region probed is uniform. The ratios are based upon the area of the Fe 2p_{3/2} iron compound peak around 711 eV and the P 2p peak. The area ratio for experiment 1 increases by about 20% in experiment 2, consistent with a film composition of iron(II) phosphate (Fe₃(PO₄)₂) in experiment 1 and iron(III) phosphate (FePO₄) in experiment 2. The area ratio for experiment 3 showed a small amount of phosphorus corresponding to a P/Fe ratio that is about 17% of that of experiments 1 and 2, consistent with a small amount of phosphate ions adsorbed on an oxide film. Bearing in mind the substantial errors involved in the area ratio

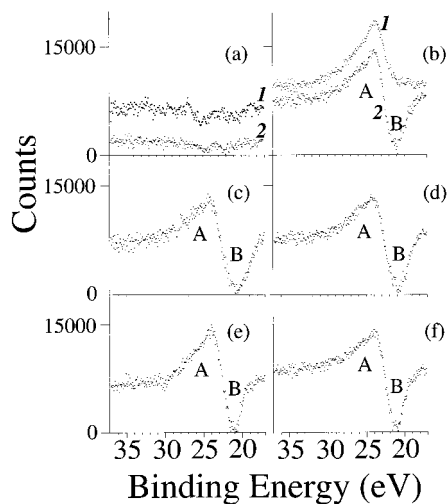


Figure 7. Difference spectra between the spectrum of the film formed after treatment in the anaerobic cell and exposure to the atmosphere for 3 months and other spectra and the spectrum of the species identified in a–h below. Each background subtracted spectrum was adjusted so that the most intense point in the spectrum was set to 10 000 counts. The spectrum subtracted is that of the film initially formed before exposure to the atmosphere in (a) **1** (where the spectrum has been shifted by 2500 counts to prevent overlap with **2**), that of FePO_4 in a-**2**. In b, **1** corresponds to the normal spectrum of the film formed after treatment in the anaerobic cell and exposure to the atmosphere for 3 months and **2** corresponds to the difference spectrum for the film formed after treatment in the anaerobic cell and exposure to the atmosphere for $\alpha\text{-Fe}_2\text{O}_3$, with (c) $\alpha\text{-FeOOH}$, (d) $\gamma\text{-FeOOH}$, (e) $\gamma\text{-Fe}_2\text{O}_3$, and (f) Fe_3O_4 . Regions A and B are identified in the text.

approach, and the clear inhomogeneous nature of the film with the presence of metal and iron satellites, we have not attempted further quantification. Atomic ratios using the O 1s region are of little value because there are additional sources of oxygen such as chemisorbed oxygen and chemisorbed water.

An estimate of the film thicknesses may be made based upon the area ratio of the Fe 2p core level features for the metal and metal compounds if one makes the crude assumption that the sample is composed of a uniform homogeneous film on top of the metal as was made for the aluminum case above. Using this assumption the thickness of the phosphate layer in experiment 1 (assumed to be Fe(II)) would be about 30 Å, and in experiment 1 the phosphate layer (assumed to be Fe(III)) would be about 60 Å thick.

3.3.2. Valence Band Spectra. Conclusive evidence for the chemical identity of the surface films formed in these experiments is again provided by valence band photoemission.

3.3.2.1. Inner Valence Band Spectra of Oxidized Iron and Iron Phosphate. Figure 7b-**1** shows the inner valence band region for the film formed after exposure of the film formed in the anaerobic cell to the atmosphere for three months and shows the difference spectra for appropriate oxidized iron species and iron phosphate. Figure 7a-**1** shows the difference spectrum for the film formed in the anaerobic cell before and after air exposure, showing little change in the region. The ability of this region to distinguish between oxidized iron species and iron(III) orthophosphate is indicated by the difference spectra shown in Figure 7. Thus while the

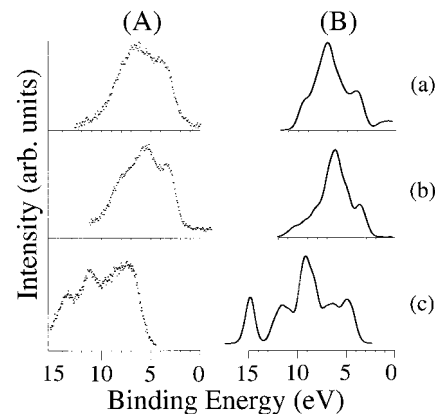


Figure 8. (A) Experimental valence band X-ray photoelectron spectra and (B) spectra calculated from band structure calculations of (a) $\alpha\text{-FeOOH}$, (b) $\alpha\text{-Fe}_2\text{O}_3$, and (c) $\text{FePO}_4\cdot 2\text{H}_2\text{O}$.

difference spectrum between the surface formed after exposure of the film formed in the anaerobic cell to the atmosphere and iron(III) orthophosphate indicates that these spectra are almost identical (Figure 7a), there are considerable differences between this spectrum and the oxidized iron species. One notes two features in the difference spectra, identified as A and B. Spectrum A arises from the P–O shoulder at around 28 eV in the orthophosphate spectra which is absent from the spectra of the oxides. Spectrum B arises from the difference in the binding energy and width of the principally O 2s region in the oxides and those of the phosphate as seen in the aluminum case. As in the aluminum case the oxyhydroxides show the greatest peak width. We have chosen Fe(III) compounds for most of the comparisons, but Fe_3O_4 (Figure 7f) and FeO (not shown) show substantial differences too.

3.3.2.2. Valence Band Spectra of Oxidized Iron and Iron Phosphate. Figure 8 presents experimental and calculated spectra of a typical iron(III) oxyhydroxide (FeOOH), iron(III) oxide (Fe_2O_3), and iron(III) phosphate ($\text{FePO}_4\cdot 2\text{H}_2\text{O}$). We have discussed the iron phosphate valence band spectra in detail elsewhere.⁵ The iron phosphate spectrum is clearly different from the oxide spectra with intense features at 11 and 14 eV which are predicted by the spectrum generated from a band structure calculation with no intensity in this region present in the oxides. We have discussed the full energy range of the oxide and oxyhydroxide spectra elsewhere.^{13,37} We have not calculated a metaphosphate spectrum for iron, but we anticipate that it will show the characteristic features found for the metaphosphate ion reported for $\text{Al}_4(\text{P}_4\text{O}_{12})_3$, especially because we have shown above that the bands for the aluminum metaphosphate are quite flat, suggesting a small cation dependence in this spectrum.

Figure 9a,b-1) presents the valence band spectrum of experiment 1. The spectrum can be seen to be quite different from that of oxidized iron and iron metaphosphate. The characteristic metaphosphate features are not seen at 16 and 11 eV, and indeed there is a valley in the spectrum in Figure 9a,b-1 at 16 eV. The features in the spectrum do seem somewhat broader than those of the iron(II) orthophosphate shown for comparison, but the peak positions correspond to orthophosphate, and the feature around 6 eV corresponds to Fe 3d intensity. Comparison of iron(II) and iron(III) orthophosphate

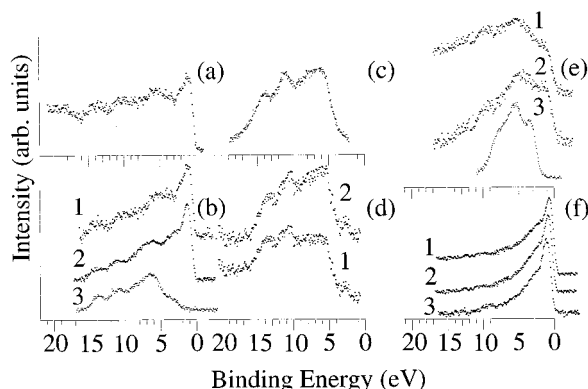
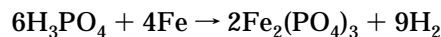


Figure 9. Valence band X-ray photoelectron spectra of (a) the film formed on argon ion etched iron metal after treatment in 5 M orthophosphoric acid in the anaerobic cell (E1); (b) the valence band region of a where 1 shows the spectrum with a nonlinear background removed (E1), A2" shows the addition of A3" and f-3 and A3" shows the valence band region of $\text{Fe}_3\text{-(PO}_4)_2\cdot 8\text{H}_2\text{O}$ with a nonlinear background removed; (c) the valence band region of $\text{FePO}_4\cdot 2\text{H}_2\text{O}$ with a nonlinear background removed; (d) the film in a after exposure to the atmosphere for 3 months (E2), where 1 shows the original data, and 2 the data with a nonlinear background removed; (e) the film formed on as received iron metal in 5 M orthophosphoric acid on the bench (E3), where 1 shows the original data, 2 the data with a nonlinear background removed, and 3 the valence band region of Fe_2O_3 with a nonlinear background removed; and (f) the film formed on argon-ion etched iron metal after exposure to deoxygenated water in the anaerobic cell for 10 min (E4), where 1 shows the original data, 2 the data with a nonlinear background removed, and 3 the valence band spectrum of iron with any oxide removed by argon-ion etching with a nonlinear background removed.

(Figure 9b-3 and Figure 8c) shows a fall in the relative intensity of the 6 eV feature consistent with the lowering of the P/Fe ratio in the high oxidation state oxide.⁵ The valence band region from experiment 1 is complicated by the presence of considerable metal evidenced by the intense metal peak around 1 eV corresponding to the iron band edge. Examination of Figure 9f-3 shows the appearance of a clean iron surface where it can be seen that there is a considerable tail on the iron peak, a characteristic feature of the valence band spectrum of unoxidized metallic iron. Figure 9b-2 shows the addition of the spectrum of unoxidized metallic iron and that of iron(II) phosphate. The spectra were added so that they were first normalized to the same number of maximum counts, and then the counts in the iron spectrum were multiplied by 3 before addition of the iron(II) phosphate spectrum. The resulting spectrum (Figure 9b-2) can be seen to approximate the main features of the spectrum from experiment 1. The valence band spectrum of the same sample after 3 months in atmosphere (experiment 2) is given in Figure 9d. For comparative purposes the spectrum of hydrated iron phosphate ($\text{FePO}_4\cdot 2\text{H}_2\text{O}$) is provided in Figure 9c. The background subtracted spectra in Figure 9c,d-2 are superimposable with the characteristic phosphate features at 11 and 14 eV, strongly suggesting that the product of experiment 2 is FePO_4 . The sharp metal edge of experiment 1 is lost in experiment 2 as a result of the thickening of the film on atmospheric exposure as was observed in the aluminum case. The thickened film is stable in atmosphere and continues to protect the underlying metal. There is *no evidence for the presence*

of metal oxide in the valence bands of experiments 1 and 2. The electrochemical treatment of iron has produced an air stable film of nonnative oxide at the electrode surface. It is clear that the phosphate film is *directly attached to the metal surface*.

This process may involve the formation of the phosphate ion in a process such as



followed by air oxidation of the $\text{Fe}_2(\text{PO}_4)_3$ to give FePO_4 . It is interesting to note that the very reactive aluminum metal initially forms metaphosphate, the less reactive copper forms both metaphosphate and phosphate initially,¹¹ and the less reactive iron forms only phosphate.

Figure 9e-1 presents the valence band data for the sample subjected to electrochemistry carried out in a conventional electrochemical cell, with the sample transferred in air to the spectrometer (experiment 3) and the 10 min deoxygenated water dip of etched iron in the anaerobic cell (experiment 4) is given in Figure 9f-1. Clearly the films formed in these situations are oxide in nature rather than phosphate. The oxidized iron shows features below 10 eV, well out of the region where the phosphate features at 11 and 14 eV are found. The background subtracted spectrum from experiment 3 (Figure 9e-2 is compared with the background subtracted spectrum of $\alpha\text{-Fe}_2\text{O}_3$ in Figure 9e-3. Comparison of the valence band of $\alpha\text{-Fe}_2\text{O}_3$ and $\alpha\text{-FeOOH}$ (Figure 7) shows that the overlap with the metal edge in experiment 3 makes it hard to distinguish the oxidized film as the oxide or oxyhydroxide, and significant amounts of the latter are likely in the aqueous environment used. The spectra are similar, with the addition of the underlying metal edge in Figure 9e-1,-2.

Experiment 4 shows a valence band spectrum characteristic of metallic iron with a very small amount of oxide. Comparison of the background subtracted spectrum in Figure 9f-2 with the spectrum of oxide free argon-ion etched metal (Figure 9f-3) shows little oxide.

4. Conclusions

Electrochemical treatment of *oxide free* ultrahigh-pressure aluminum and iron electrodes at -0.7V or the rest potential (which is close to -0.5V in both cases) for 10 min in 5.0 M phosphoric acid results in phosphate films with thicknesses on the order of the original native oxide. The phosphated surfaces are air stable and *directly attached to the respective metal surface in the absence of oxide*. These are believed to be the first examples of metals present in air with some film other than native oxide. The identity of the films could be conclusively determined by valence band XPS. Identical electrochemical experiments on an as received ultrahigh-pressure aluminum and iron samples led to an oxide surface with little adsorbed phosphate ions.

Acknowledgment. This material is based upon work supported by the National Science Foundation under Grant No. CHE-9421068. The U.S. Government has certain rights in this material.